

Calculation of the Specific Heat for the II-III and II-IV Phase Transitions in NH_4Br

H. Yurtseven^a and A. Mertoglu

*Department of Physics, Istanbul Technical University,
Maslak, Istanbul – Turkey*

(Received February 26, 2001)

The specific heat C_{V1} is calculated in this study using the prediction of an Ising model for the II-III phase transition at 0.05 GPa and for the II-IV phase transition at the pressures of 0.19, 0.99 and 2.1 GPa close to T_C for the NH_4Br crystal. The values of the critical exponent for the specific heat of NH_4Br which we determine from our analysis, are close to the predicted values of $1/16$ ($T < T_C$) and $1/8$ ($T > T_C$) obtained from the 3d Ising model. Our calculated specific heat C_{V1} agrees well with the experimental C_P below T_C in the antiferro-ordered (phase III) and ferro-ordered (phase IV) phases of NH_4Br . Above T_C (disordered phase II) there occur discrepancies between our calculated C_{V1} and the observed C_P for NH_4Br .

PACS. 63.70.+h – Statistical mechanics of lattice vibrations and displacive phase transitions.

I. Introduction

NH_4Br exhibits a λ -type of phase transition at 234 K ($P = 0$). This transition occurs from the disordered $\bar{1}$ phase (phase II) to the antiferro-ordered $^\circ$ phase (phase III), as the temperature decreases from high temperatures. As the temperature decreases further, the antiferro-ordered $^\circ$ phase transforms into the ordered \pm phase (phase IV). All these phase transformations occur at zero pressure. In the disordered $\bar{1}$ phase, which has a CsCl type crystal structure with O_h^1 symmetry, the ammonium ions are randomly distributed between two energetically equivalent states [1]. In the antiferro-ordered $^\circ$ phase the NH_4^+ tetrahedra have an anti-parallel arrangement in the a-b plane and they tend to orientate along the c-axis. This phase has a tetragonal structure with D_{4h} symmetry, whereas the ferro-ordered \pm phase has a CsCl structure with T_d^1 symmetry, in which all the NH_4^+ ions are parallel to each other.

As the pressure increases from the atmospheric pressure, there occur phase transformations between the disordered $\bar{1}$, antiferro-ordered $^\circ$ and the ordered \pm phases in the NH_4Br crystal. There also occur phase transformations between the $\bar{1}$, $^\circ$ and \pm phases in NH_4Br , as the concentration varies with the temperature. Various P-T and X-T phase diagrams for ammonium and deuterio-ammonium bromide have been given in the literature. The first experimental P-T phase diagram of ammonium halides was obtained [2] and it has been modified [3]. A general P-T phase diagram in ammonium and deuterio-ammonium halides, which locate the tricritical and multi-critical points on the disordered $\bar{1}$ and ferro-ordered \pm phase line, has also been reported [4]. The T-X phase diagrams for the $\text{NH}_4\text{Br}_x\text{Cl}_{1-x}$ system have been given as experimental studies in the literature [5-8]. Some theoretical phase diagrams in ammonium halides have also been introduced in previous

studies [9-11]. Recently, we have obtained the P-T phase diagram of ammonium halides using mean field theory [12]. More recently, we have also obtained the T- X_{Br} phase diagram for the $\text{NH}_4\text{Br}_x\text{Cl}_{1-x}$ system [13].

The α -phase transitions in NH_4Br have been studied extensively using various experimental techniques [14-20] and also some theoretical methods [9, 21-23]. We have reviewed some of those studies and we have calculated the Raman frequencies of some lattice modes using the observed volume data for NH_4Br [24].

The α -phase transition in NH_4Br can also be studied by calculating its specific heat. In our previous study [25] we have developed an Ising model superimposed on an Einstein and/or Debye model. By applying this model to the ammonium halides, we have been able to calculate the specific heat C_{V1} due to the nearest-neighbour spin interactions using our observed Raman frequencies in the NH_4Cl system [26, 27] at zero pressure. At higher pressures, we have applied our model to the NH_4Cl system to calculate the specific heat C_{V1} for its tricritical and second order phase transitions by analysing our observed Raman frequencies [27, 28]. We have also applied an Ising model to NH_4Br to calculate the specific heat C_{V1} close to its α -phase transition at zero pressure, using our observed Raman frequencies in this crystalline system [28, 29].

In this study we calculate the specific heat C_{V1} on the basis of the Ising model by directly analyzing the experimentally measured C_P data [20] for the II-III phase transition at the pressure of 0.05 GPa and for the II-IV phase transition at the pressures of 0.19, 0.99, and 2.1 GPa in the NH_4Br crystal. We determine the values of the critical exponent a for the specific heat for each pressure condition, which are close to the predictions of a 3d Ising model.

In Section 2 we give an outline of the theory. In Section 3 we present our calculations and results. Our discussion is given in Section 4. Finally, conclusions are given in Section 5.

II. Theory

The Ising Hamiltonian of a system can be written as

$$H_I = J(V) \sum_{ij} \frac{1}{2} (s_i + s_j); \quad (1)$$

where s_i and s_j are the Ising spin variables for the nearest-neighbour interactions and $J(V)$ is the exchange integral depending upon the volume.

The free energy of this system having the Ising Hamiltonian is defined as

$$F_I(J(V); T) = -kT \ln Z(J(V); T); \quad (2)$$

where \ln is the logarithm of the partition function defined as

$$Z = \sum_{ij} e^{-H_I/kT}; \quad (3)$$

Since the specific heat is the second derivative of the free energy, we then have

$$C_{V1} = k \frac{\partial^2 F_I}{\partial (kT)^2}; \quad (4)$$

where $\partial^2 \phi / \partial (J/kT)^2$ denotes the second derivative of ϕ with respect to $J=kT$. Eq. (4) is the analytical expression of the specific heat C_V for an Ising system.

The divergence behaviour of the specific heat C_{V1} can be obtained from the power-law formula for the free energy,

$$F_1 = A_0^0 + A^0 j^{2/a}; \quad (5)$$

where a is the critical exponent for the specific heat, A_0^0 and A^0 are the parameters defined as $A_0^0 = JA_0$ and $A^0 = JA$. Here A_0 and A are dimensionless constants. In Eq. (5) the reduced temperature is $j = T - T_C / T_C$, where T_C is the critical temperature. By taking the second derivative of ϕ with respect to $J=kT$ according to Eq. (2), where we use Eq. (5), we get the power-law formula for the specific heat (Eq. 4):

$$C_{V1} = j JA \frac{T}{T_C} (1 - a)(2 - a) j^{1/a}; \quad (6)$$

In order to obtain Eq. (6), we neglect the $j^{1/a}$ term which diverges weakly near T_C .

III. Calculations and results

We calculated here the specific heat C_{V1} according to the prediction of an Ising model (Eq. (6)) using the observed C_P data [20] for the II-III phase transition at 0.05 GPa pressure and for the II-IV phase transition at the pressures of 0.19, 0.99 and 2.1 GPa in NH_4Br .

III-1. II-III Phase Transition of NH_4Br at 0.05 GPa

For the phase transition from phase II (disordered $\bar{}$) to phase III (antiferro-ordered $^\circ$) in the NH_4Br crystal, we fitted Eq. (6) to the experimentally observed C_P data at $P = 0.05$ GPa [20], below and above the critical temperature ($T_C = 226$ K). From our analysis, we obtained the value of the critical exponent, $a = 0.06$ for the specific heat and $JA = j 632.75 \text{ J mol}^{-1}$ for $T < T_C$. Above the critical temperature ($T > T_C$) our analysis gave us the values of $a = 0.11$ and $JA = j 461.99 \text{ J mol}^{-1}$, as given in Table I. By assuming that the values a and JA do not vary in the phases of II and III, respectively, we were able to predict the specific heat C_{V1} using Eq. (6). We plot our calculated C_{V1} with the observed C_P data [20] as a function of temperature at $P = 0.05$ GPa for NH_4Br ($T_C = 226$ K) above T_C (phase II) and below T_C (phase III) in Fig. 1.

III-2. II-IV phase transition of NH_4Br at 0.19 GPa

We fitted Eq. (6) to the observed C_P data [20] at $P = 0.19$ GPa ($T_C = 208.7$ K) for II-IV (disordered $\bar{}$ -ferro-ordered \pm) phase transition in NH_4Br above and below T_C . From this fitting, we obtained the value of $a = 0.10$ as the critical exponent for the specific heat and the value of $JA = j 547.58 \text{ J mol}^{-1}$ for $T < T_C$. Also, we obtained that $a = 0.16$ and $JA = j 410.85 \text{ J mol}^{-1}$ for $T > T_C$, according to Eq. (6), as is also given in Table I. By taking those values of a and JA as constants in the phases of II and IV, respectively, we then calculated the specific heat C_{V1} according to Eq. (6). We give our plot of C_{V1} versus T , with the C_P data [20] at $P = 0.19$ GPa ($T_C = 208.7$ K) above T_C (phase II) and below T_C (phase IV) of NH_4Br in Fig. 2.

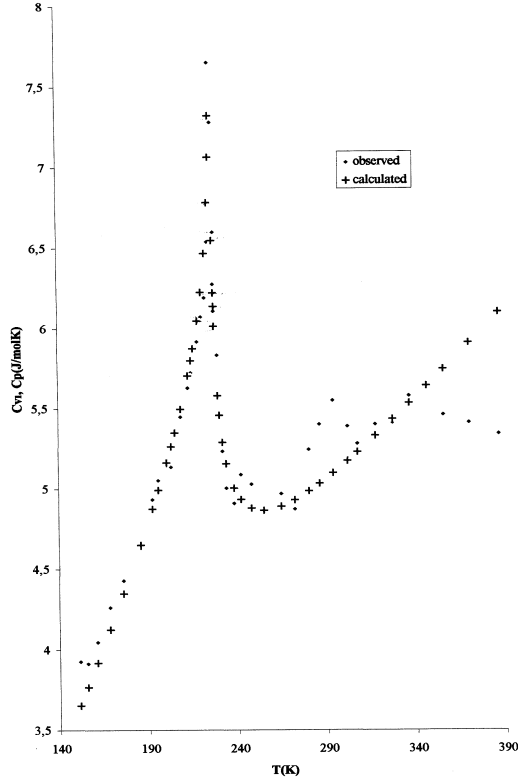


FIG. 1. Our calculated C_{V1} (Eq. (6)) as a function of temperature at 0.05 GPa for the II-III phase transition in NH_4Br ($T_C = 226$ K). The experimental C_P data shown here are taken from Ref. [20].

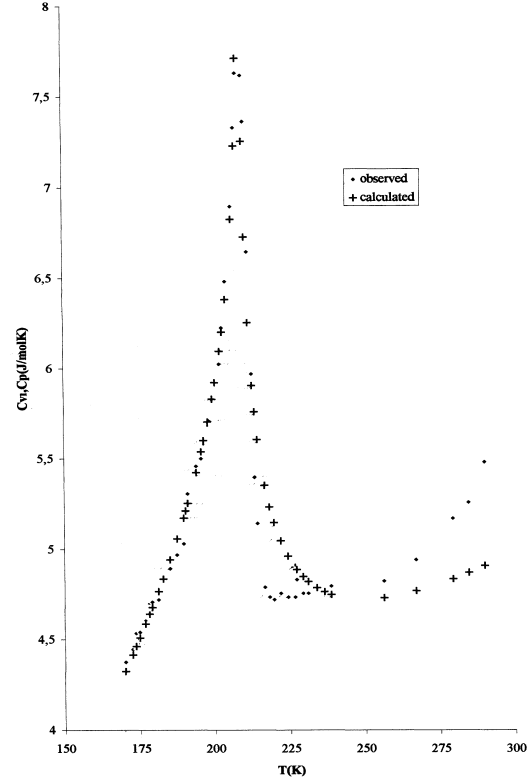


FIG. 2. Our calculated C_{V1} (Eq. (6)) as a function of temperature at 0.19 GPa for the II-IV phase transition in NH_4Br ($T_C = 208.7$ K). The experimental C_P data shown here are taken from Ref. [20].

TABLE I. Our values of the critical exponent \mathbf{a} for the specific heat and the \mathbf{JA} values (Eq. (6)) for the II-III phase transition (0.05 GPa) and II-IV phase transition (0.19, 0.99 and 2.1 GPa) in NH_4Br .

P(GPa)	T_C (K)	$T < T_C$		$T > T_C$	
		\mathbf{a}	$\mathbf{j JA}(\text{Jmol}^{-1})$	\mathbf{a}	$\mathbf{j JA}(\text{Jmol}^{-1})$
0.05	226.0	0.06	632.75	0.11	461.99
0.19	208.7	0.10	547.58	0.16	410.85
0.99	249.5	0.08	771.98	0.15	516.29
2.1	280.4	0.05	954.41	0.18	577.47

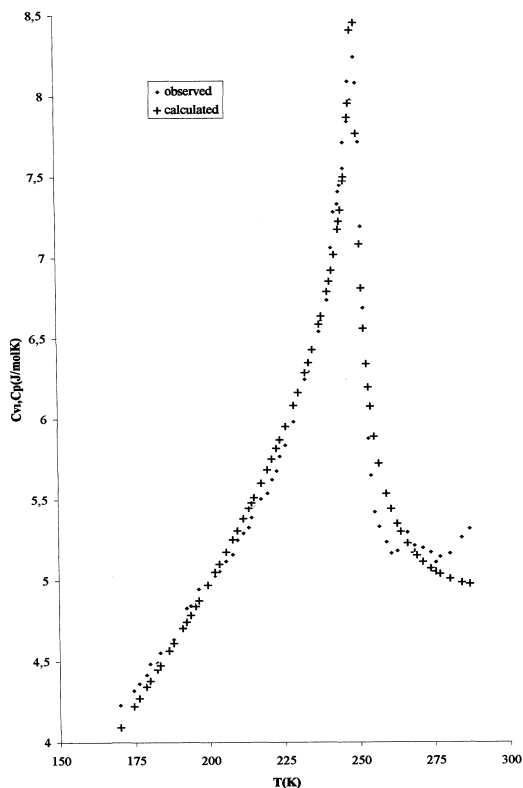


FIG. 3. Our calculated C_{V1} (Eq. (6)) as a function of temperature at 0.99 GPa for the II-IV phase transition in NH_4Br ($T_C = 249.5$ K). The experimental C_P data shown here are taken from Ref. [20].

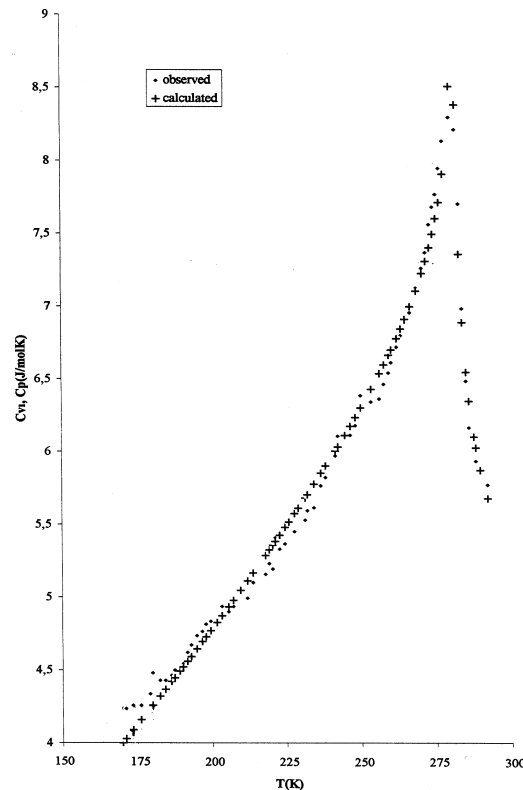


FIG. 4. Our calculated C_{V1} (Eq. (6)) as a function of temperature at 2.1 GPa for the II-IV phase transition in NH_4Br ($T_C = 280.4$ K). The experimental C_P data shown here are taken from Ref. [20].

III-3. II-IV phase transition of NH_4Br at 0.99 GPa

We also analysed the II-IV phase transition in NH_4Br at the pressure of $P = 0.99$ GPa by means of Eq. (6) using the literature C_P data [20]. This analysis gave us the values of $\mathbf{a} = 0.08$ and $JA = \int 771.98 \text{ J mol}^{-1}$ for $T < T_C$ and also $\mathbf{a} = 0.15$ and $JA = \int 516.29 \text{ J mol}^{-1}$ for $T > T_C$, where $T_C = 249.5$ K. Our values of \mathbf{a} and JA are tabulated in Table I. We assumed here that our values of \mathbf{a} and JA remain constant in the phases II and IV, respectively. Under this assumption, we calculated the specific heat C_{V1} using Eq. (6). Our calculated C_{V1} and the observed C_P data [20] are plotted against the temperature for the II-IV phase transition at $P = 0.99$ GPa ($T_C = 249.5$ K) for NH_4Br in Fig. 3

III-4. II-IV phase transition of NH_4Br at 2.1 GPa

We performed the same analysis for the II-IV phase transition at $P = 2.1$ GPa using the C_P data [20] for NH_4Br . From our fitting (Eq. (6)), we had the exponent value of $\mathbf{a} = 0.05$ and $JA = \int 954.41 \text{ J mol}^{-1}$ ($T < T_C$), the values of $\mathbf{a} = 0.18$ and $JA = \int 577.47 \text{ J mol}^{-1}$ ($T > T_C$),

where $T_C = 280.4$ K for the NH_4Br crystal. Those values are given in Table I. We then used those constant values of a and JA to calculate the specific heat C_{V1} according to Eq. (6). We plot our calculated specific heat C_{V1} and the observed C_P data [20] as a function of temperature at $P = 2.1$ GPa for NH_4Br in Fig. 4.

IV. Discussion

We calculated here the specific heat C_{V1} using Eq. (6) predicted by an Ising model, as a function of temperature for the II-III phase transition at 0.05 GPa (Fig. 1) and for the II-IV phase transitions at the pressures of 0.19 GPa (Fig. 2), 0.99 GPa (Fig. 3) and 2.1 GPa (Fig. 4) in the NH_4Br crystal. For this calculation, we first determined the values of the critical exponent a and JA by fitting Eq. (6) to the experimental C_P data for each constant pressure above and below T_C . Using the constant values of those fitting parameters, we then calculated the specific heat C_{V1} according to Eq. (6), as indicated above. Our calculated C_{V1} is in good agreement with the observed C_P data below T_C for the II-III and II-IV phase transitions which in fact, seems to emerge at ≈ 235 K, as shown in Fig. 1.

For the II-IV phase transition in NH_4Br at the pressures of 0.19, 0.99 and 2.1 GPa, the values of the critical exponent, namely, 0.10, 0.08 and 0.05 (Table I) below T_C describe satisfactorily the observed behaviour of C_P , according to Eq. (6), as seen in Figs. 2-4, respectively. Above T_C we have the exponent values of 0.16, 0.15 and 0.18 for the pressures of 0.19, 0.99, and 2.1 GPa, respectively, which seem to describe the critical behaviour of the specific heat less satisfactorily. In fact, for the temperatures far away from T_C in the disordered phase II, as indicated above, Eq. (6) is no longer valid. Thus, regarding our exponent values (Table I), the value of ≈ 0.1 describes the critical behaviour in NH_4Br as seen from Figs. 1-4. Above T_C our calculated C_{V1} agrees with the C_P data up to the temperatures of nearly $T_C + 50$ K for the pressures of 0.05 GPa (Fig. 1) and 0.19 GPa (Fig. 2), whereas for 0.99 GPa (Fig. 3) and 2.1 GPa (Fig. 4) this agreement is valid up to nearly $T_C + 30$ K and $T_C + 10$ K, respectively, according to the experimental C_P data available. In fact, the critical exponent a describes the critical behaviour of C_{V1} close to T_C , according to Eq. (6). It seems that for the II-III phase transition in NH_4Br ($P = 0.05$ GPa), our value of $a = 0.06$ below T_C (Table I) describes this critical behaviour of C_{V1} satisfactorily, whereas above T_C our value of $a = 0.11$ (Table I) describes the observed behaviour C_P reasonably well, up to ≈ 275 K. Above this temperature, we get oscillations in C_{V1} and C_P for the II-III phase transition (from the disordered $\bar{}$ phase to the antiferro-ordered $^\circ$ phase) in NH_4Br . Also, the value between 0.1 and 0.2 describes the critical behaviour of C_{V1} and C_P for the II-IV phase transition (from the disordered $\bar{}$ phase to the ferro-ordered \pm phase) in NH_4Br . Disagreement between our calculated C_{V1} and the observed C_P [20] at the high temperatures, as indicated above T_C (Figs. 1-4), may be attributed to the disordering effects which emerge due to the random orientations of the NH_4^+ ions.

Our values between 0.1 and 0.2 for the critical exponent a which describes the divergence behaviour of the specific heat C_{V1} and C_P of NH_4Br , can be compared with the predicted values of 0.066 (1/16) for $T < T_C$ and 0.125 (1/8) for $T > T_C$ due to a 3d Ising model. So, the II-III and II-IV phase transitions in NH_4Br can be explained by a power-law formula (Eq. (6)) predicted by an Ising model.

We also note here that we compared our calculated C_{V1} with the experimentally measured C_P data. In fact, we initially used the C_P data to calculate C_{V1} . Close to T_C , the specific

heat C_V diverges, whereas C_P remains constant but it shows anomalous behaviour close to T_C according to an Ising model superimposed on an Einstein and/or Debye model which we have developed [25]. Thus, it is convenient to fit the C_V expression (Eq. (6)) to the experimentally measured C_P , so that the critical behaviour of both C_{V1} and C_P close to T_C can be seen from Figs. 1-4.

V. Conclusions

We calculated here the specific heat C_{V1} predicted by an Ising model for the II-III and II-IV phase transitions of NH_4Br under constant pressures. By fitting our C_{V1} expression to the experimental C_P data, we determined the values of the critical exponent which describes the divergence behaviour of the specific heat close to T_C . Our calculated C_{V1} from our analysis is in very good agreement with the observed C_P below T_C for the II-III and II-IV phase transitions in NH_4Br . Above T_C , the agreement is less satisfactory. This indicates that our method of calculating the specific heat for an Ising model is reasonable, it explains the observed behaviour of the NH_4Br crystal for the phase transitions considered.

References

- [1] H. A. Levy and S. W. Peterson, Phys. Rev. **83**, 766 (1952).
- [2] R. Stevenson, J. Chem. Phys. **34**, 346 (1961).
- [3] W. Press *et al.*, Phys. Rev. **B14**, 1983 (1976).
- [4] R. C. Leung, C. Zahradnik and C. W. Garland, Phys. Rev. **B19**, 2612 (1979).
- [5] I. R. Jahn and E. Neumann, Solid State Comm. **12**, 721 (1973).
- [6] C. W. Garland, R. C. Leung and C. Zahradnik, J. Chem. Phys. **71**, 3158 (1979).
- [7] T. Goto, T. Fujimura, K. Kamiyoshi, Phys. Stat. Solidi (a) **45**, 513 (1978).
- [8] M. Yoshizawa *et al.*, J. Phys. C: Solid State Phys. **16**, 131 (1983).
- [9] Y. Yamada, M. Mori and Y. Noda, J. Phys. Soc. Jpn. **32**, 1565 (1972).
- [10] A. Hüller, Z. Physik, **270**, 343 (1974).
- [11] V. G. Vaks and V. E. Schneider, Phys. Stat. Solidi (a) **35**, 61 (1976).
- [12] H. Yurtseven, S. Salihoglu and A. Tüblek, Phase Trans. **54**, 1 (1995).
- [13] Ö. Tari, H. Yurtseven and S. Salihoglu, Phase Trans. **72**, 351 (2000).
- [14] C. W. Garland and J. F. Yarnell, J. Chem. Phys. **44**, 1112 (1966).
- [15] C. W. Garland and R. A. Young, J. Chem. Phys. **49**, 5282 (1968).
- [16] C. H. Wang, Phys. Rev. Lett. **26**, 1226 (1971).
- [17] G. Egert, I. R. Jahn and D. Renz, Solid State Comm. **9**, 775 (1971).
- [18] C. H. Wang and R. B. Wright, J. Chem. Phys. **57**, 4401 (1972).
- [19] H. Yamashita and I. Tatsuzaki, J. Phys. Soc. Jpn. **53**, 2075 (1984).
- [20] R. G. Ross and P. Andersson, J. Phys. C: Solid State Phys. **20**, 4745 (1987).
- [21] T. Geisel and J. Keller, J. Chem. Phys. **62**, 3777 (1975).
- [22] M. Matsushita, J. Chem. Phys. **65**, 23 (1976).
- [23] H. Yurtseven, M. Güleç and W. F. Sherman, Phase Trans. **56**, 137 (1996).

- [24] H. Yurtseven and W. F. Sherman, Phase Trans. **54**, 1 (1995).
- [25] H. Yurtseven, Phase Trans **47**, 59 (1994).
- [26] H. Yurtseven and W. F. Sherman, Phase Trans. **47**, 69 (1994).
- [27] H. Yurtseven, D. Kayışoglu and W. F. Sherman, Phase Trans. **67**, 399 (1998).
- [28] H. Yurtseven and A. Yanik, J. Mol. Struc. **553**, 267 (2000).
- [29] H. Yurtseven, A. Yanik and W. F. Sherman, Mod. Phys. Lett. **B12**, 1089 (1998).